


## Compact NbN resonators with high kinetic inductance

Xing-Yu Wei(魏兴雨), Jia-Zheng Pan(潘佳政), Ya-Peng Lu(卢亚鹏), Jun-Liang Jiang(江俊良), Zi-Shuo Li(李子硕), Sheng Lu(卢盛), Xue-Cou Tu(涂学凑), Qing-Yuan Zhao(赵清源), Xiao-Qing Jia(贾小氢), Lin Kang(康琳), Jian Chen(陈健), Chun-Hai Cao(曹春海), Hua-Bing Wang(王华兵), Wei-Wei Xu(许伟伟), Guo-Zhu Sun(孙国柱), and Pei-Heng Wu(吴培亨)

**Citation:**Chin. Phys. B, 2020, 29 (**12**): 128401. DOI: 10.1088/1674-1056/abc2b8
Journal homepage: http://cpb.iphy.ac.cn; http://iopscience.iop.org/cpb

**What follows is a list of articles you may be interested in**

---

## The coupling effect of air-bridges on broadband spiral inductors in SiC-based MMIC technology

Jia-Xin Zheng(郑佳欣), Xiao-Hua Ma(马晓华), Yang Lu(卢阳), Bo-Chao Zhao(赵博超), Heng-Shuang Zhang(张恒爽), Meng Zhang(张濛), Li-Xiang Chen(陈丽香), Qing Zhu(朱青), Yue Hao(郝跃)
Chin. Phys. B, 2017, 26 (**8**): 088401. DOI: 10.1088/1674-1056/26/8/088401

## Negative-index dispersion and accidental mode degeneracy inan asymmetric spoof–insulator–spoof waveguide

Li-li Tian(田莉莉), Jian-long Liu(刘建龙), Ke-ya Zhou(周可雅), Yang Gao(高扬), Shu-tian Liu(刘树田)
Chin. Phys. B, 2017, 26 (**7**): 078401. DOI: 10.1088/1674-1056/26/7/078401

## Multi-mode coupling analysis of a sub-terahertz band planar corrugated Bragg reflector

Liu Guo, Luo Yong, Wang Jian-Xun, Shu Guo-Xiang
Chin. Phys. B, 2015, 24 (**11**): 118403. DOI: 10.1088/1674-1056/24/11/118403

## Analysis of the third harmonic for class-F power amplifiers with an *I–V* knee effect

Zhao Bo-Chao, Lu Yang, Wei Jia-Xing, Dong Liang, Wang Yi, Cao Meng-Yi, Ma Xiao-Hua, Hao Yue
Chin. Phys. B, 2015, 24 (**5**): 058401. DOI: 10.1088/1674-1056/24/5/058401

## Complete eigenmode analysis of a ladder-type multiple-gap resonant cavity

Zhang Chang-Qing, Ruan Cun-Jun, Zhao Ding, Wang Shu-Zhong, Yang Xiu-Dong
Chin. Phys. B, 2014, 23 (**8**): 088401. DOI: 10.1088/1674-1056/23/8/088401

---

RAPID COMMUNICATION

# Compact NbN resonators with high kinetic inductance*

Xing-Yu Wei(魏兴雨)[1,2], Jia-Zheng Pan(潘佳政)[1,2], Ya-Peng Lu(卢亚鹏)[1,2], Jun-Liang Jiang(江俊良)[1,2], Zi-Shuo Li(李子硕)[1,2], Sheng Lu(卢盛)[1,2], Xue-Cou Tu(涂学凑)[1,2], Qing-Yuan Zhao(赵清源)[1,2], Xiao-Qing Jia(贾小氢)[1,2], Lin Kang(康琳)[1,2], Jian Chen(陈健)[1,2], Chun-Hai Cao(曹春海)[1], Hua-Bing Wang(王华兵)[1,2], Wei-Wei Xu(许伟伟)[1], Guo-Zhu Sun(孙国柱)[1,2,†], and Pei-Heng Wu(吴培亨)[1,2]

[1] *Research Institute of Superconductor Electronics, School of Electronic Science and Engineering, Nanjing University, Nanjing* 210093, *China*
[2] *Purple Mountain Laboratories, Nanjing* 211111, *China*

(Received 24 August 2020; revised manuscript received 2 October 2020; accepted manuscript online 20 October 2020)

We design and fabricate $\lambda/2$ coplanar waveguide NbN resonators, the thickness and length of which are only several nanometers and hundred microns, respectively. The quality factor of such compact resonators can reach up to $7.5 \times 10^4$ at single photon power level at 30 mK with the resonance frequency around 6.835 GHz. In order to tune the resonant frequency, the resonator is terminated to the ground with a dc-SQUID. By tuning the magnetic flux in the dc-SQUID, the effective inductance of the dc-SQUID is varied, which leads to the change in the resonant frequency of the resonator. The tunability range is more than 30 MHz and the quality factor is about $3 \times 10^3$. These compact and tunable NbN resonators have potential applications in the quantum information processing, such as in the precision measurement, coupling and/or reading out the quantum states of qubits.

**Keywords:** superconducting resonator, NbN, kinetic inductance, tunable resonator

**PACS:** 84.40.Dc, 85.25.Dq **DOI:** 10.1088/1674-1056/abc2b8

Superconducting qubit[1–4] is one of the most attractive research subjects in the past decades due to its promising potential applications in the quantum information processing. The most recent progress in superconducting qubit is the demonstration of quantum supremacy[5] with more than 50 qubits on a quantum chip. The more qubits a quantum computer has, the more powerful it is. However, considerable parts of the area in the superconducting quantum circuits are usually occupied by superconducting resonators. These superconducting resonators have been extensively applied to the superconducting quantum circuits and are indispensable tools for reading out and/or coupling the quantum states of qubits.[6–9] If the size of the superconducting resonators can be reduced, the integration of the superconducting qubit circuits can be greatly improved. Various methods have been developed to improve the integration of the quantum circuits. One of them is to take advantage of the kinetic inductance,[10] which is an intrinsic property of superconductors.

As one of the type-II superconductors, niobium nitride (NbN) film with several nanometer thickness has high kinetic inductance. Such NbN film has a lot of successful applications such as being photon detectors[11,12] and super-inductors.[13] Here we present a superconducting circuit consisting of NbN resonator with thickness of several nanometers. Compared with the superconducting resonators with normal thickness, our NbN superconducting resonator has a high kinetic inductance and can shorten the length of the resonator by more than 10 times in the microwave band (4–10 GHz), which can greatly save the space of the readout and/or coupling circuits of qubits. Furthermore, we also present a tunable NbN superconducting resonator with a dc-SQUID embedded. The tunable range of frequency is over 30 MHz and the loaded quality factor is around $3 \times 10^3$ at zero flux bias. The NbN film in our devices is approximately 6 nm thick, which is deposited on a high-resistance silicon wafer by magnetron sputtering technique. With electron beam lithography and reactive ion etching, three reflective half-wavelength coplanar waveguide (CPW) resonators are fabricated as shown in Fig. 1(a). In order to match the characteristic impedance of the resonator to minimize the transmission losses, a narrowing transmission line known as Klopfenstein taper is designed with the impedance of 50 Ω in the input and output ports. Each resonator is coupled to the middle of the taper line by a capacitance $C_k$ (Fig. 1(b)) and the other end of the resonator is open (Fig. 1(c)).

In a CPW resonator, the characteristic impedance is defined as $Z_0 = \sqrt{L_l/C_l}$, where $C_l$ and $L_l$ are the capacitance and inductance per unit length of the resonator, respectively. The first resonance mode of our resonator is $l = \lambda/2$, where $l$ is the length of the resonator. The corresponding resonance fre-

*Project partially supported by the National Key R&D Program of China (Grant No. 2016YFA0301801), the National Natural Science Foundation of China (Grant Nos. 11474154 and 61521001), PAPD, Dengfeng Project B of Nanjing University, and the Fundamental Research Funds for the Central Universities, China (Grant No. 14380134).

†Corresponding author. E-mail: gzsun@nju.edu.cn

© 2020 Chinese Physical Society and IOP Publishing Ltd 

quency is $\omega_r = \pi/\sqrt{L_r C_r}$, where $L_r = L_l \times l$ and $C_r = C_l \times l$ are the total inductance and capacitance of the resonator, respectively. Generally speaking, for superconductors, the inductance $L_l = L_g + L_k$, in which $L_g$ is the temperature-independent geometric inductance and $L_k$ is the temperature-dependent kinetic inductance.[14] $L_k$ is related to the inertia of moving Cooper pairs and can contribute significantly to $L_l$ due to the suppressed resistivity and thus the large charge carrier relaxation time. We have[15]

$$L_{k0} = \hbar R/[\pi \Delta(0)], \tag{1}$$

where $R$ is the normal state sheet resistance and can be obtained by fitting the $R$–$T$ data (as shown in Fig. 2(a)), $\hbar$ is the reduced Planck constant, and $\Delta(0)$ is the superconducting gap at zero temperature. NbN is experimentally found to be a strongly coupled superconductor with $\Delta(0) = 2.08\ k_B T_c$,[16] where $k_B$ is the Boltzmann constant and $T_c$ is the superconducting critical temperature. From the experimental data, we obtain $L_{k0} \approx 132$ (pH/sq). For a 1 μm wide nanowire, the corresponding kinetic inductance per unit length is $L_k = 1.32 \times 10^{-4}$ (H/m), $L_g$ is about $1 \times 10^{-6}$ (H/m). Because $L_g$ is two orders of magnitude smaller than $L_k$, we can legitimate the assumption $L_l \approx L_k$.

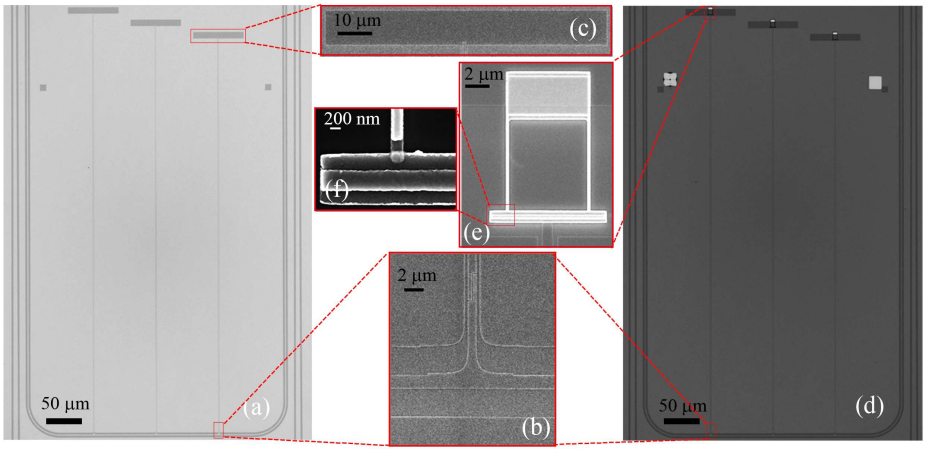



**Fig. 1.** (a) Micrograph of three coplanar waveguide (CPW) resonators coupled to a taper line. (b) Scan electron micrograph (SEM) of the coupling capacitance $C_k$. (c) SEM of the end of a resonator. (d) Micrograph of three CPW resonators with dc-SQUIDs. (e) SEM of a dc-SQUID. (f) SEM of a Josephson junction in the dc-SQUID.

The loaded quality factor $Q_l$ of the resonator is a parallel combination of the internal $Q_i$ and external quality factors $Q_e$,[17,18]

$$\frac{1}{Q_l} = \frac{1}{Q_e} + \frac{1}{Q_i}, \tag{2}$$

$$Q_e = \frac{\pi(1 + R_0^2 C_k^2 \omega_r^2)}{2 Z_0 R_0 C_k^2 \omega_r^2}. \tag{3}$$

The $Q_e$ results from the coupling of the resonator to the taper line through capacitance $C_k$. $R_0 = 570\ \Omega$ is the characteristic impedance of the resonator. $Z_0 = 50\ \Omega$ is the input impedance. $Q_i$ is determined by the intrinsic losses of the resonator.[19] In our devices, $C_k = 0.7$ fF. This coupling capacitance is so small that the resonators are all in the under-coupled regime, which means $Q_e \gg Q_i$ and $Q_l \approx Q_i$. Our sample is located in an Oxford Triton dilution refrigerator with magnetic shielding. The transmission characteristics of the sample are measured with a vector network analyzer (VNA). The input signal from the VNA is heavily attenuated at different temperature stages in order to minimize the environmental noise and ensure the input signal into the sample at single photon level power. The output signal from the sample is passed through several cryogenic circulators and amplified by a high-electron-mobility transistor (HEMT) amplifier located in the dilution refrigerator and other amplifiers at room temperature. Low-pass filters are put in both the input and output lines. RC filters and copper-powder filters are used in the flux bias line,[20] with which an external magnetic field is applied to a dc-SQUID (Fig. 1(e)) described in detail in the following.

A strip of NbN film with the thickness of 6 nm is measured to obtain its dependance of resistance on the temperature ($R$–$T$) (as shown in Fig. 2(a)). By fitting the data with the following equation proposed by Aslamasov and Larkin:[15]

$$\sigma(T) = \sigma_n + \frac{e^2 T_c}{16 \hbar d (T - T_c)}, \quad (T > T_c), \tag{4}$$

we get the normal-state sheet resistance $R = 959.87\ \Omega$ and superconducting critical temperature $T_c = 8.5$ K, from which we obtain $L_{k0} \approx 132$ (pH/sq) according to Eq. (1). In Eq. (4), $e$ is the electron charge, $d$ is the thickness of the film, and $\sigma_n = 1.736 \times 10^5$ (S/m) is the normal state conductivity.

Figure 2(b) shows the microwave transmission characteristic $S_{21}$ of a resonator with $l = 641$ μm, from which we obtain the resonant frequency $f_r \approx 6.835$ GHz and the internal quality factor $Q_i \approx 7.5 \times 10^4$. The average photon number in the resonator is given by $\langle n \rangle = Z_{in} Q_l^2 P_{in}/h\pi^2 Z_0 f_r^2 Q_e$.[11] Here the average photon number $\langle n \rangle$ in the resonator is set to about 1 by reducing the input microwave power and the temperature is

$T = 30$ mK.

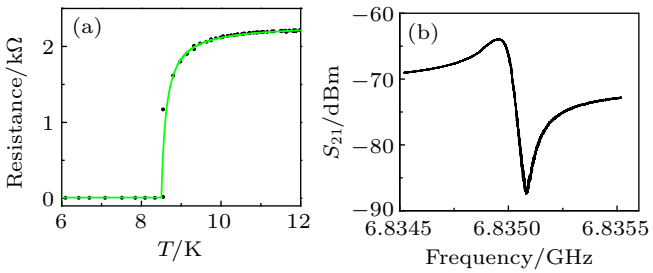



**Fig. 2.** (a) The $R$–$T$ of a NbN film. Dots are the experimental data and the green line is the calculated result with Eq. (4). $T_c = 8.5$ K. (b) Transmission characteristic curve $S_{21}$ of one superconducting NbN resonator.

Then we vary the temperature and obtain the dependence of $f_r$ and $Q_i$ on the temperature (see Fig. 3(a)). The variation of $f_r$ is mainly attributed to two mechanisms. One is the two-level systems (TLSs) in the amorphous materials. These TLSs result in the temperature-dependent variation of the dielectric constant and cause the increase of $f_r$ and $Q_i$ as shown by the following equations:

$$\frac{f_r(T)-f_r(0)}{f_r(0)} = \frac{F\delta_{TLS}^{i}}{\pi}\left[\mathrm{Re}\,\Psi\left(\frac{1}{2}-\frac{hf_r(0)}{2\pi i k_B T}\right) - \ln\frac{hf_r(0)}{2\pi k_B T}\right], \tag{5}$$

$$\frac{1}{Q_i(T)}-\frac{1}{Q_i(0)} = F\delta_{TLS}^{i}\tanh\left(\frac{hf_r(0)}{2k_B T}\right), \tag{6}$$

where $\Psi$ is the complex digamma function, $F$ is the filling factor, and $F\delta_{TLS}^{i}$ is the intrinsic loss tangent. This mechanism dominates when $T$ is low.[21]

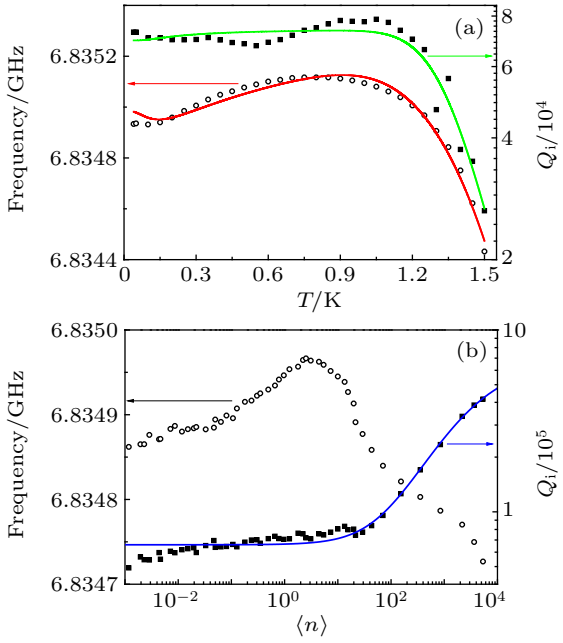



**Fig. 3.** (a) Resonant frequency $f_r$ (circles) and $Q_i$ (squares) versus temperature from 30 mK to 1.5 K. Red line is the fitted result using weighted Eqs. (5) and (7). Green line is the fitted result using weighted Eqs. (6) and (8). (b) Resonant frequency $f_r$ (circles) and $Q_i$ (squares) versus average photon number in the resonator. Blue line is the fitted result using Eq. (9).

The other mechanism is the temperature-dependent variation of conductivity of the NbN film when $T < T_c$. This mechanism dominates when $T$ is high.[22] According to the Mattis–Bardeen theory, the conductivity of the NbN film will change with temperature as follows:

$$\frac{\Delta f_r}{f_r} = -\frac{\alpha}{2}\frac{\Delta X_s(T)}{X_s} = \frac{\alpha}{2}\frac{\Delta\sigma_2(T)}{\sigma_n}, \tag{7}$$

$$\Delta\frac{1}{Q_i} = \alpha\frac{\Delta R_s(T)}{X_s} = -\alpha\frac{\Delta\sigma_1(T)}{\sigma_n}, \tag{8}$$

where $R_s$ ($X_s$) is the surface resistance (inductance) of the NbN film and $\sigma_1$ ($\sigma_2$) is the real (imaginary) part of conductivity of the NbN film. The kinetic inductance fraction $\alpha$ is defined as the ratio of the kinetic inductance to the total inductance and $\sigma_n$ is the normal state conductivity.[23]

The dependance of $f_r$ and $Q_i$ on the average number of photons $\langle n\rangle$ in the resonator is demonstrated in Fig. 3(b). $f_r$ decreases as $\langle n\rangle$ increases when $\langle n\rangle > 1$. This is mainly attributed to the change of the kinetic inductance, which has a Duffing-like non-linear behavior.[24] $Q_i$ of the resonator gradually increases from $5\times10^4$ when $\langle n\rangle$ is between $10^{-3}$ and $10^2$. This is a representation of depolarization of TLSs, which can be fitted with the TLS loss model described by[25]

$$\frac{1}{Q_i} = F\delta_{TLS}^{0}\frac{\tanh(hf/2k_B T)}{(1+\langle n\rangle/n_c)^{\beta}} + \frac{1}{Q_0}, \tag{9}$$

where $n_c = 65.76$ is the number of photons equivalent to the saturation field of TLSs, $Q_0 = 6.75\times10^5$ is the quality factor of the other loss mechanism, and $\beta = 0.618$ describes the strength of TLS saturation with power. $F\delta_{TLS}^{0} = 1.37\times10^{-5}$ is the TLS loss tangent, which is temperature- and power-independent. When $\langle n\rangle > 10^2$, $Q_i$ significantly increases as $\langle n\rangle$ increases, which is consistent with the Duffing non-linearity.

To tune the resonant frequency of the resonator, it is terminated by a dc-SQUID. Such dc-SQUID is a superconducting loop intersected by two nominally identical Josephson junctions (see Figs. 1(d)–1(f)). The dc-SQUID acts as a non-linear inductance element in quantum circuits[26] and the corresponding inductance $L_s$ depends on the superconducing critical current $I_c$ and the magnetic flux $\Phi$ through the superconducting loop

$$L_s(\Phi) = \frac{\Phi_0}{2\pi I_c|\cos(\pi\Phi/\Phi_0)|}, \tag{10}$$

where $\Phi_0 = h/2e$ is the flux quantum. Thus the total inductance of the resonator with a dc-SQUID in serial is $L = L_r + L_s(\Phi)$.

Then the resonant frequency of the tunable half-wavelength resonator is

$$\omega(\Phi) = \pi/\sqrt{(L_s(\Phi)+L_r)C_r}. \tag{11}$$

In order to demonstrate the tunability of the resonator, a dc current is applied to a superconducting coil on the sample

box to vary the flux bias threading the dc-SQUID while measuring the resonate frequency $f_r$ simultaneously.

We show the dependence of $f_r$ on the normalized flux bias when $\langle n \rangle \approx 1$. $f_r$ changes periodically with the flux bias and can be fitted well by the equation

$$f_r(\Phi) = \frac{1}{2\sqrt{\left[\dfrac{\Phi_0}{2\pi I_c|\cos(\pi\Phi/\Phi_0)|} + L_r\right]C_r}}. \tag{12}$$

The tunable frequency range is over 30 MHz. The range can be adjusted by controlling $I_c$, which is mainly determined by the barrier in the Josephson junctions.[27]

The flux-dependent $Q_i$ in one period is shown in Fig. 4(b). The internal quality factor is about $3 \times 10^3$ at $\Phi = 0$. Compared with the resonator without a dc-SQUID, $Q_i$ decreases dramatically. Due to the effect of subgap resistance in the junctions of the dc-SQUID,[28] $Q_i$ decreases as the resonator is detuned from $\Phi/\Phi_0 = 0$. The sudden decrease of $Q_i$ around $\Phi/\Phi_0 = \pm 0.25$ may be due to the energy dissipation caused by the microwave photon transitions between the resonator and defects in the Josephson junctions of the dc-SQUID.[29–31]

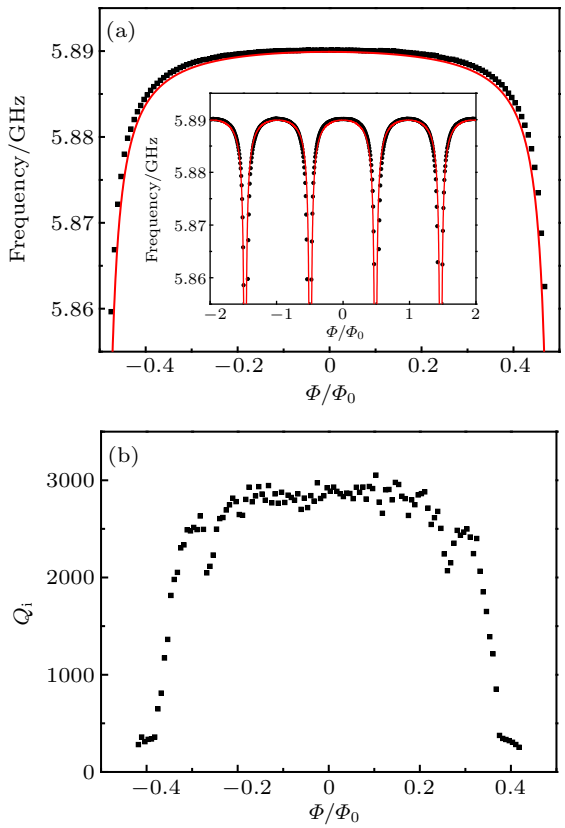



**Fig. 4.** (a) The $f_r$ versus the normalized flux bias $\Phi/\Phi_0$ through the dc-SQUID. The red line represents the fitted result with $I_c = 4.96$ μA, $L_r = 84.6$ nH, $C_r = 85.0$ fF. The hollow circles represent the experiment data. The inset shows the periodical dependance of $f_r$ on $\Phi/\Phi_0$. (b) $Q_i$ of the resonator versus $\Phi/\Phi_0$ in one period.

In summary, we have successfully fabricated compact superconducting NbN resonators with thickness of several nanometers. The internal quality factor $Q_i$ reaches $7.5 \times 10^4$ at single photon power level at 30 mK, which is higher than that reported in the previous work.[13] In order to further improve the quality factor, one may use the substrate with lower loss and/or improve the quality of the NbN film. By terminating the resonator by a dc-SQUID, we have experimentally demonstrated a tunable superconducting NbN resonator with tunable range of frequency over 30 MHz and $Q_i$ around $3 \times 10^3$ at $\Phi/\Phi_0 = 0$. To the best of our knowledge, this is the first report about a tunable NbN resonator with thickness of several nanometers. Larger tunable range of the resonant frequency may be obtained by optimizing the parameters of the SQUID. The length of these resonators is only hundreds of microns due to the high kinetic inductance of the NbN film with thickness of several nanometers. This provides a promising material to improve the integration of quantum circuits by reducing the size of the readout and coupling resonators usually used in the superconducting qubits. Also such devices may be implemented in the precision measurement such as photon detection.

## References


[1] Nakamura Y, Pashkin Y A and Tsai J S 1999 *Nature* **398** 786

[2] Vion D, Aassime A, Cottet A, Joyez P, Pothier H, Urbina C, Esteve D and Devoret M H 2002 *Science* **296** 886

[3] Martinis J M, Nam S, Aumentado J and Urbina C 2002 *Phys. Rev. Lett.* **89** 117901

[4] Chiorescu I, Nakamura Y, Harmans C J P M and J E Mooij 2003 *Science* **299** 1869

[5] Arute F, Arya K, Babbush R, *et al* 2019 *Nature* **574** 505

[6] Wallraff A, Schuster D I, Blais A, and Frunzio L, Huang R S, Majer J, Kumar S, Girvin S M and Schoelkopf R J 2004 *Nature* **431** 162

[7] Blais A, Huang R S, Wallraff A, Girvin S M and Schoelkopf R J 2004 *Phys. Rev. A* **69** 062320

[8] Ashhab S, You J Q and Nori F 2009 *Phys. Rev. A* **79** 032317

[9] Siddiqi I, Vijay R, Metcalfe M, Boaknin E and Devoret M H 2005 *Phys. Rev. B* **73** 054510

[10] Leduc H G, Bumble B, Day P K, Eom B H, Gao J, Golwala S, Mazin B A, McHugh S, Merrill A, Moore D C, Noroozian O, Turner A D and Zmuidzinas J 2010 *Appl. Phys. Lett.* **97** 102509

[11] Goltsman G N, Okunev O, Chulkova G, Lipatov A, Semenov A, Smirnov K, Voronov B, Dzardanov A, Williams C and Sobolewski R 2001 *Appl. Phys. Lett.* **79** 705

[12] Sobolewski R, Verevkin A, Gol'tsman G N, Lipatov A and Wilsher K 2003 *IEEE Trans. Appl. Supercond.* **13** 1151

[13] Niepce D, Burnett J and Bylander J 2019 *Phys. Rev. A* **11** 044014

[14] Watanabe K, Yoshida K, Aoki T and Kohjiro S 1994 *Jpn. J. Appl. Phys.* **33** 5708

[15] Tinkham M 1996 *Physics Today* **49** 74

[16] Mondal M, Kamlapure A, Chand M, Saraswat G, Kumar S, Jesudasan J, Benfatto L, Tripathi V and Raychaudhuri P 2011 *Phys. Rev. Lett.* **106** 047001

[17] Pozar D M 1993 *Microwave Engineering* (Addison Wesley Publishing Company)

[18] Goppl M, Fragner A, Baur M, Bianchetti R, Filip P S, Fink J M, Leek P J, Puebla G, Steffen L andWallraf A 2008 *J. Appl. Phys.* **104** 113904

[19] Oconnell A D, Ansmann M, Bialczak R C, Hofheinz M, Katz N, Lucero E, Mckenney C, Neeley M, Wang H, Weig E M, Cleland A N and Martinis J M 2008 *Appl. Phys. Lett.* **92** 112903

[20] Pan J, Jooya H Z, Sun G, Fan Y, Wu P, Telnov D A, Chu S and Han S 2017 *Phys. Rev. B* **96** 174518

[21] Gao J, Daal M, Anastasios V, Shwetank K, Jonas Z, Bernard S, Benjamin A M, Peter K D and Henry G L 2008 *Appl. Phys. Lett.* **92** 152505

[22] Mattis D C and Bardeen J 1958 *Phys. Rev.* **111** 412

[23] Gao J 2008 *The Physics of Superconducting Microwave Resonators* (Ph.D. Thesis) (California: California Institute of Technology Pasadena)

[24] Swenson L J, Day P K, Eom B H, Leduc H J, Llombart N, Mckenney C M, Noroozian O and Zmuidzinas J 2013 *J. Appl. Phys.* **113** 104501

[25] Burnett J, Sagar J, Kennedy O W, Warburton P A and Fenton J C 2017 *Phys. Rev. Appl.* **8** 014039

[26] Palacios-Laloy A, Nguyen F, Mallet F, Bertet P, Vion D and Esteve D 2008 *Journal of Low Temperature Physics* **151** 1034

[27] Ambegaokar V and Baratoff A 1963 *Phys. Rev. Lett.* **11** 104

[28] Sandberg M, Wilson C M, Persson F, Bauch T, Johansson G, Shumeiko V, Duty T and Delsing P 2008 *Appl. Phys. Lett.* **92** 203501

[29] Simmonds R W, Lang K M, Hite D A, Nam S, Pappas D P and Martinis J M 2004 *Phys. Rev. Lett.* **93** 077003

[30] Sun G, Wen X, Mao B, Zhou Z, Yu Y, Wu P and Han S 2010 *Phys. Rev. B* **82** 132501

[31] Sun G, Wen X, Mao B, Chen J, Yu Y, Wu P and Han S 2010 *Nat. Commun.* **1** 51